Appl. Math. and Comp. Sci., 1998, Vol.8, No.1, 39–50

A POLAR COORDINATE BASED SLIDING MODE DESIGN FOR VIBRATION CONTROL

K. DAVID YOUNG*

A polar coordinate based sliding mode control design approach for solving vibration control problems is proposed. The phase plane in subdivided into multiple sets, and a different sliding manifold can be chosen for each of the sets. This flexibility in the design allows a different variable structure control law to be applied depending on the phase angle of the vibration. Transient performance improvements over conventional VSC with sliding hyperplanes are demonstrated.

1. Introduction

In sliding mode design, the sliding manifold is typically defined as the intersection of linear hyperplanes of the state space of the plant (Utkin, 1977; 1992). While this design approach is appealing due to the linear space characteristics of the sliding manifold which allow the use of linear control design tools to optimize the sliding mode dynamics, it is generally difficult to restrict sliding mode to occur only in some subsets of the state space. Such design requirements arise in vibration control where often it is desirable to restrict motion only in certain preferred directions due to physical constraints (Young, 1993). In this paper, we propose a sliding mode design approach which is based on polar coordinates of the phase space in mechanical systems, encountered in vibration control problems.

2. A Single DOF Oscillator Illustration

We shall introduce this design approach with the sliding mode design for a simple oscillator plant

$$\ddot{x} + kx = u \tag{1}$$

where $x, \dot{x}$ denote the position and velocity, respectively, and u represents the generalized force which is also the control input. The natural frequency of this oscillator is $\sqrt{k}$, and the bounds on the uncertain stiffness k can be estimated as $k_l \le k \le k_u$. In a typical sliding mode design, the sliding manifold is given by

$$s(x, \dot{x}) = \dot{x} + cx = 0, \qquad c > 0 \tag{2}$$

* Lawrence Livermore National Laboratory, University of California, P.O. Box 808, L–471, Livermore, California, 94551–0808, USA, e-mail: kkdyoung@llnl.gov.

resulting in a first order, stable sliding mode dynamics

$$\dot{x} = -cx \tag{3}$$

The design problem becomes complicated when the constraint $x \geq 0$ is enforced. If the sliding mode reaching condition $\dot{s}s < 0$ is to be met, the phase trajectory for initial conditions such that $x(t_0) \geq 0$, $\dot{x}(t_0) > 0$, may enter the inadmissible region $x < 0$. Although it is possible to enforce the reaching condition selectively such that the phase trajectory avoids this region, however, for such situations, it would be desirable to design a sliding manifold which excludes the inadmissible region of the phase space entirely, i.e., the set

$$S_{x \geq 0} = \{x | \, \dot{x} + cx = 0, \; x \geq 0\} \tag{4}$$

This can be accomplished by introducing polar coordinates r and θ

$$x = r\sin\theta, \qquad \dot{x} = r\cos\theta \tag{5}$$

and constructing a sliding manifold in the form

$$s(\theta) = \theta - \theta_d = 0 \tag{6}$$

Note that the phase trajectory is associated with the complex phasor

$$\vec{r} \triangleq re^{\jmath\theta} = x + \jmath\dot{x}, \qquad r = (x^2 + \dot{x}^2)^{1/2} \tag{7}$$

where r is the magnitude, and θ is the phase angle. Convergence to the equilibrium is governed by the variable r, whereas the oscillatory behavior is dictated by the variable θ.

On the sliding manifold $\theta = \theta_d$, dynamics are expected to depend on the constant parameter θ_d. Furthermore, by using the method of equivalent control to eliminate the variable θ, the sliding mode dynamics are reduced to first order,

$$\dot{r} = \tan(\theta_d)r \tag{8}$$

Since θ_d is a real constant, stability of sliding mode is guaranteed in the second and fourth quadrant of the phase plane, corresponding to $-\pi/2 < \theta_d < 0$ and $\pi/2 < \theta_d < 3\pi/2$, respectively. This should not be surprising since it is well known that the sliding line for a second order system must have negative slopes. That the classical sliding line is further subdivided into two possible, and separate sliding manifolds in the (r, θ) space is an interesting result.

3. Polar Coordinate Based Sliding Mode

The above result for single degree-of-freedom mechanical systems can be generalized to multiple degrees-of-freedom mechanical systems of the form,

$$M\ddot{x}_m + B_m\dot{x}_m + K_m x_m = u_m, \qquad x_m \in \mathbb{R}^m, \quad u_m \in \mathbb{R}^m \tag{9}$$

where the generalized mass matrix is positive definite, $M > 0$, the stiffness matrix is positive semi-definite, $K_m > 0$, and Raleigh damping is assumed, i.e.,

$$B_m = \alpha M + \beta K_m, \qquad 0 < \alpha < 1, \quad 0 < \beta < 1 \tag{10}$$

For all practical purposes, we shall deal with a mass normalized system where the state space model corresponding to (9) is given by

$$\dot{x}_1 = x_2, \qquad x_1 \in \mathbb{R}^m, \quad x_2 \in \mathbb{R}^m \tag{11}$$

$$\dot{x}_2 = -Kx_1 - \epsilon B x_2 + u, \qquad K > 0, \quad B > 0, \quad u \in \mathbb{R}^m \tag{12}$$

Note that in order to exhibit the intentional vibrational characteristics, ϵ should be sufficiently small such that the roots of $\det(\lambda^2 I + \epsilon B\lambda + K) = 0$ are complex.

Using the phasor representation, we express the generalized displacement and velocity of each mechanical degree-of-freedom in the form,

$$\vec{r}_i = r_i e^{\jmath\theta_i}, \qquad i = 1, \ldots, m \tag{13}$$

and introduce the following notations

$$r = \left[r_1, \ldots, r_m\right]^T, \qquad R \triangleq \text{diag}(r_1, \ldots, r_m) \tag{14}$$

$$\theta = \left[\theta_1, \ldots, \theta_m\right]^T, \quad c_\theta \triangleq \left[\cos\theta_1, \ldots, \cos\theta_m\right]^T, \quad s_\theta \triangleq \left[\sin\theta_1, \ldots, \sin\theta_m\right]^T \tag{15}$$

$$C_\theta \triangleq \text{diag}(\cos\theta_1, \ldots, \cos\theta_m), \qquad S_\theta \triangleq \text{diag}(\sin\theta_1, \ldots, \sin\theta_m) \tag{16}$$

to facilitate the following vectorized polar coordinate form of the states:

$$x_1 = Rc_\theta, \qquad x_2 = Rs_\theta \tag{17}$$

3.1. Sliding Mode Dynamics in Half Spaces

The sliding mode manifold is chosen as

$$\sigma = \theta - \theta_d = 0, \qquad \theta \in \mathbb{R}^m, \ \sigma = \left[\sigma_1, \ldots, \sigma_m\right]^T \tag{18}$$

and $\theta_d \in \mathbb{R}^m$ is a constant vector. The sliding mode dynamics on eqn. (18) are derivable using the method of equivalent control:

$$\dot{\theta} = -S_\theta R^{-1} x_2 + C_\theta R^{-1}[-Kx_1 - \epsilon B x_2 + u_{eq}] = 0 \tag{19}$$

which, upon simplifications yield the equivalent control,

$$u_{eq} = (T_\theta + \epsilon B)x_2 + Kx_1, \qquad T_\theta \triangleq \text{diag}(\tan\theta_1, \ldots, \tan\theta_m) \tag{20}$$

On the manifold, dynamics are of m-th order, and since T_θ is a diagonal matrix, they are decoupled,

$$\dot{r} = T_\theta\big|_{\theta=\theta_d} r \tag{21}$$

Furthermore, sliding mode is asymptotically stable if and only if

$$\theta_d^i < 0 \quad \text{or} \quad \theta_d^i \pm \pi\big|_{\theta_d^i<0}, \qquad i = 1,\dots,m, \ \ \theta_d^T = [\theta_d^1,\dots,\theta_d^m] \tag{22}$$

This implies that stable sliding mode manifolds are defined in the half spaces $P_i^+ \cap V_i^-$ and $P_i^- \cap V_i^+$ where

$$P_i^+ \triangleq \{x_1^i | \ x_1^i \geq 0\}, \qquad P_i^- \triangleq \{x_1^i | \ x_1^i < 0\}, \qquad i = 1,\dots,m \tag{23}$$

$$V_i^+ \triangleq \{x_2^i | \ x_2^i \geq 0\}, \qquad V_i^- \triangleq \{x_2^i | \ x_2^i < 0\}, \qquad i = 1,\dots,m \tag{24}$$

$$x_1^T = [x_1^1,\dots,x_1^m], \qquad x_2^T = [x_2^1,\dots,x_2^m] \tag{25}$$

whereas sliding mode manifolds in the other two half spaces $P_i^+ \cap V_i^+$ and $P_i^- \cap V_i^-$ are unstable.

3.2. Variable Structure Control Design

In the process of designing the variable structure control such that sliding mode occurs on polar coordinate based manifolds, we encounter a number of interesting design options which are directly related to the dynamic behavior outside the manifold. The equation governing the dynamics outside the manifold is given by

$$\dot{\theta} = -S_\theta s_\theta - C_\theta R^{-1}[KRc_\theta + \epsilon BRs_\theta - u] \tag{26}$$

If the stiffness and damping matrices are known, then having a perfect compensating component,

$$u^{pc} = KRc_\theta + \epsilon BRs_\theta \tag{27}$$

$$u = u^{pc} + u^a \tag{28}$$

reduce (26) to

$$\dot{\theta} = -S_\theta s_\theta + C_\theta R^{-1} u^a \tag{29}$$

Since S_θ, C_θ and R are diagonal, the dynamics outside the manifold are decoupled,

$$\dot{\theta}_i = -s\theta_i^2 + \frac{c\theta_i}{r_i} u_i^a, \qquad i = 1,\dots,m \tag{30}$$

$$s\theta_i \triangleq \sin\theta_i, \qquad c\theta_i \triangleq \cos\theta_i \tag{31}$$

Note that in contrast to a sliding mode manifold chosen as the intersection of hyperplanes in the (x_1, x_2) space where a sufficiently large relay component can be effective in ensuring that the system's trajectory converges to the manifold, a relay component in the current design does not guarantee convergence. From the above equation, it is clear that for any constant $\bar{u}$, the relay control component $u_i^a = \bar{u}\mathrm{sgn}(\sigma_i)$ does not guarantee $\dot{\sigma}_i\sigma_i < 0$. Another crucial observation is that for $\sigma_i > 0$, if $u_i^a = 0$, then

$\dot{\sigma}_i < 0$, and the manifold $\sigma_i = 0$ is reached from above. So the design is focused on a feedback control for $\sigma_i < 0$. Let

$$u_i^a = \begin{cases} \bar{u} r_i c\theta_i, & \bar{u} > 0 \quad \text{if} \quad \sigma_i < 0 \\ 0 & \quad\quad\quad \text{if} \quad \sigma_i \geq 0 \end{cases} \tag{32}$$

The value for $\bar{u}$ such that $\dot{\sigma}_i < 0$ is determined from the expression

$$\bar{u}_c = \tan^2 \theta_c^i \tag{33}$$

where θ_c^i denotes the critical value for θ_i such that the condition $\dot{\sigma}_i = 0$ is satisfied. Note that the magnitude of the corresponding $\bar{u}_c$ increases monotonically with $|\theta_c^i|$, and is unbounded for $\theta_c^i = \pm\pi/2$. Clearly, it is impossible to satisfy the sliding mode reaching condition for $\sigma_i < 0$ near the vertical axis of the phase plane (θ_i, r_i). A practical solution is to estimate the largest permissible value for $\bar{u}$ from the bounds on the control variables. Although this design would not satisfy the reaching condition for some conic sector near the vertical axis, we can subdivide the phase plane into two sets:

$$\Theta_i^+ = \left\{(\theta_i, r_i) \mid \theta_c^i + \frac{\pi}{2} \geq \theta_i \geq -\theta_c^i,\ 0 \leq r_i < \infty\right\} \tag{34}$$

$$\Theta_i^- = \left\{(\theta_i, r_i) \mid \theta_c^i + \frac{\pi}{2} < \theta_i < \frac{3\pi}{2} + \theta_c^i,\ 0 \leq r_i < \infty\right\} \tag{35}$$

with

$$0 < \theta_c^i < \frac{\pi}{2}, \qquad |\theta_d^i| < \theta_c^i \tag{36}$$

For the set Θ_i^+, we choose the sliding mode manifold $\sigma_i = 0$ with $\theta_d^i = -|\theta_d^i|$, i.e., $\sigma_i^+ = \theta_i + |\theta_d^i| = 0$, and for the set Θ_i^-, we choose $\theta_d^i = |\theta_d^i| + \pi/2$, and define the manifold as $\sigma_i^- = \theta_i - |\theta_d^i| - \pi/2 = 0$. With this assignment of different sliding mode manifolds for the two different sets, the conic sector for which the reaching condition is not satisfied for one of the sliding mode manifold falls into a region for which the reaching condition is satisfied for the complementary choice of sliding mode manifold. These two sets and their corresponding sliding mode manifolds are depicted in Fig. 1.

The remaining task is to replace the u^{pc} component with a design which does not require precise information on the stiffness and damping matrices. We first assume that the stiffness matrix is composed of a nominal $\bar{K}$ and an uncertain part K^u. Let

$$u^{pc} = \bar{K} R c_\theta - G^* R c_\theta - C^* R s_\theta \tag{37}$$

where $G^* \in \mathbb{R}^{m \times m}$ and $C^* \in \mathbb{R}^{m \times sm}$ are variable structure feedback gain matrices whose ij-th element is of the form

$$[G^*]_{ij} = g_{ij}^* \mathrm{sgn}(c\theta_i)\mathrm{sgn}(c\theta_j)\mathrm{sgn}(\sigma_i), \quad [C^*]_{ij} = c_{ij}^* \mathrm{sgn}(c\theta_i)\mathrm{sgn}(s\theta_j)\mathrm{sgn}(\sigma_i) \tag{38}$$

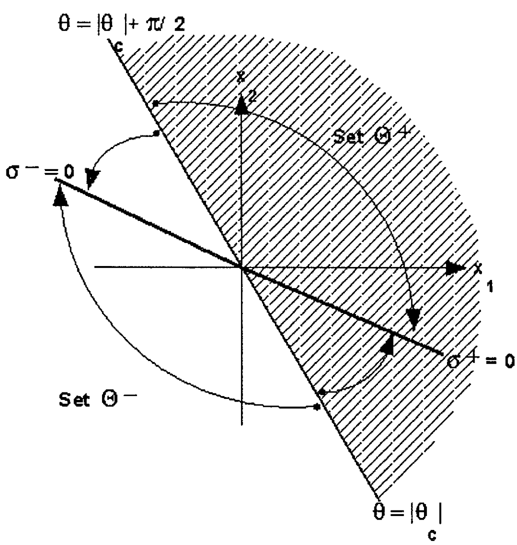

Fig. 1. Choice of different sliding mode manifolds for different sets.

where the scalar gain parameters are chosen to satisfy the inequalities

$$g^*_{ij} > \left|k^u_{ij}\right|, \qquad c^*_{ij} > \epsilon b_{ij} \tag{39}$$

where k^u_{ij} and b_{ij} are the ij-th elements of K^u and B respectively. The variable structure control which guarantees that

$$\dot{\sigma}_i \sigma_i < 0, \qquad i = 1, \ldots, m \tag{40}$$

can be written comprehensively as

$$u = U_c x_1 + \bar{K} x_1 - G^* x_1 - C^* x_2, \quad U_c \triangleq \mathrm{diag}(\bar{u}^1_c, \ldots, \bar{u}^m_c) \tag{41}$$

$$\bar{u}^i_c = \begin{cases} \bar{u}_c & \text{if } \sigma_i < 0 \\ 0 & \text{if } \sigma_i \geq 0 \end{cases}, \quad i = 1, \ldots, m \tag{42}$$

3.3. Coupled Sliding Mode Dynamics

It is possible to generalize the above design such that the sliding mode dynamics are coupled. In (17), replace the diagonal matrix R by NR, where N is a nonsingular matrix, i.e.,

$$x_1 = NRc_\theta, \qquad x_2 = NRs_\theta \tag{43}$$

Another possible modification is on the parameterization of the sliding manifold. Instead of (18), let

$$\sigma = \theta - F\theta_d = 0 \tag{44}$$

where F is a nonsingular matrix. Dynamics on this manifold are given by

$$\dot{r} = N^{-1}T_\theta \big|_{\theta = F\theta_d} r \tag{45}$$

Clearly, given a desired sliding manifold dynamics characterized by a Hurwitz matrix Γ, it is unnecessary to invoke the additional parameterizations in the matrix F. For example, we can choose $F = I$, and for any nonsingular Γ, let

$$N = T_\theta \big|_{\theta = \theta_d} \Gamma^{-1} \tag{46}$$

Note that a nondiagonal matrix N is still required to couple the sliding mode dynamics. The seemingly uncoupled sliding mode manifold with $F = I$ is implicitly coupled with respect to the physical phase angles, since

$$\theta_i = \tan^{-1}\left(\frac{n_i^T x_2}{n_i^T x_1}\right), \qquad i = 1, \dots, m \tag{47}$$

where n_i^T denotes the i-th row of N.

4. Benchmark Comparison with Classical Sliding Mode

We shall examine the characteristics of the polar coordinate based sliding mode design by applying the design approach to a simple vibration control problem, and comparing the dynamic responses of the resulting feedback system with a sliding mode controller which is designed using the classical sliding hyperplanes in the phase space.

4.1. The Vibration Control Problem Description

An active vibration control system for a platform typically used in high precision manufacturing can be modeled with the following second order dynamics:

$$m\ddot{x} + b_s\dot{x} + k_s x = f + mg \tag{48}$$

where g is the gravitational constant, k_s stands for the stiffness, b_s denotes the damping coefficient of the spring support, and f is the active force applied to the platform. Figure 2 shows a schematic diagram of this system where the reference to the unsprung length of the spring from which the displacement of the platform is measured is indicated. The spring support is designed to take compressive load only, thus $x \geq 0$ is a physical constraint. The equilibrium $\bar{x} = mg/k_s$ can be removed by defining the state variables

$$x_1 = x - \bar{x}, \qquad x_2 = \dot{x} \tag{49}$$

and by defining

$$b = \frac{b_s}{m}, \qquad k = \frac{k_s}{m}, \qquad u = \frac{f}{m} \tag{50}$$

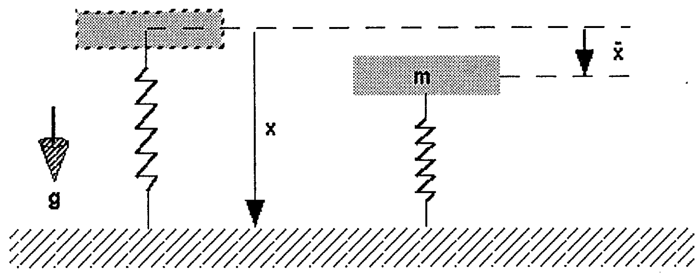

Fig. 2. Vibratory platform schematic diagram.

the dynamics in (48) are reduced to the standard form. Clearly, if additional mass is loading the platform, the natural frequency of the system $\sqrt{k}$ decreases. So unknown mass loading is a practical issue, however, maximum loading which is often included in the rating of the platform is specified. Note that in the standard form, the control variable is expressed in Newtons per unit mass, making the design scalable for different size platform design. The numerical values for this design are chosen to be

$$b = 0.04\pi, \qquad k = 4\pi^2 \tag{51}$$

corresponding to a resonant frequency of 1 Hz.

4.2. Polar Coordinate Based Sliding Mode

The desired phase angle θ_d is chosen to be $\pi/4$ corresponding to a one second time constant motion on the sliding manifold. Following the design procedures in the last section, we subdivide the phase plane into two sets by choosing the value of the critical angle θ_c. We let $\theta_c = 3\pi/8$, and according to (33), $\bar{u}_c = 5.83$. The two sets $\Theta^+ = 0$ and $\Theta^- = 0$ are separated by the line $s_c = x_2 + \tan(3\pi/8)x_1 = 0$. The variable structure control can be designed as an on-off Pulse-Width-Modulation controller,

$$u = \begin{cases} kx_1 + bx_2 + +\bar{u}_c x_1 & \text{if } \sigma^+ < 0 \text{ or } \sigma^- > 0 \\ 0 & \text{if } \sigma^+ \geq 0 \text{ or } \sigma^- \leq 0 \end{cases} \tag{52}$$

where

$$\theta = \tan^{-1}\left(\frac{x_2}{x_1}\right) \tag{53}$$

$$\sigma^+ = \theta + \frac{\pi}{4} = 0, \qquad \sigma^- = \theta + \frac{3\pi}{4} = 0 \tag{54}$$

Note that the exact values of the platform's parameters are assumed known, and this information is used in this controller as feedback compensation. Clearly, we can introduce additional terms in this controller to mitigate the effects of the parametric uncertainties, we keep this controller simple so that we can make more effective benchmark comparisons with the classical hyperplane based sliding mode design. Implementation of this controller also requires measurement of θ, the detection of the phase trajectory with respect to the two sets, and the signs of the switching functions σ^+ and σ^-. Given x_1 and x_2, these implementation issues are readily solved with additional logics to resolve the sign ambiguity and modulus 2π nature of any phase angle measurements.

4.3. Classical Hyperplane Based Sliding Mode Design

When a hyperplane in the phase space is chosen as the sliding mode manifold,

$$s = x_2 + cx_1 = 0 \tag{55}$$

we choose a variable structure control in the form

$$u = kx_1 + bx_2 - \big(g|x_2| + h\big)\mathrm{sgn}(s) \tag{56}$$

For benchmarking purposes, we let $c = 1$ so that sliding mode on $s = 0$ also has a one second time constant, and with $g = 1.1$ and $h = 1$, reaching of the manifold $s = 0$ is guaranteed for the dynamics in (48), and for any point on the phase space.

4.4. Dynamic Performance Evaluations

The two sliding mode control designs are evaluated using two test cases, both of which include a pulse load introduced at 2 seconds for 0.1 seconds. For the first test case, the initial conditions place the phase point just inside the Θ^+ set, whereas for the second case, it is just inside the Θ^- set. These tests are chosen to illustrate the selective switching behavior of the sliding mode manifolds in response to dynamic loadings typically found in vibration control. The position and velocity measurements are recorded for four seconds in all cases. The phase trajectories of these two cases when a polar coordinate based sliding mode control design is used are shown in Figs. 3 and 4. In Case 1, the manifold $\sigma^+ = 0$ is active and the phase trajectory is driven such that sliding mode occurs. Before sliding mode on this manifold reaches the equilibrium $\bar{x}$ or the origin of the phase space, the platform is excited by the pulse load, and since the VSC is not designed to reject it, sliding mode is destroyed and the phase trajectory is in the set Θ^- when the pulse load expires. A different manifold $\sigma^- = 0$ becomes active, and as before sliding mode occurs on this second manifold. A similar sequence of events takes place for Case 2 except sliding mode occurs on $\sigma^- = 0$ before the pulse load, and on $\sigma^+ = 0$ after.

The same initial conditions and pulse loads for the two test cases are applied for the variable structure control which is based on the classical hyperplane design. The respective phase trajectories are shown in Figs. 5 and 6. In both cases, sliding mode occurs on $s = 0$ before the pulse load. However, at the end of the four-second period, the phase trajectories are still in their reaching phases. We note that the behavior outside the sliding manifold is identical as expected since there is only one sliding manifold regardless of the location of the phase point. This is most clearly shown in Fig. 6 where the slopes of the phase trajectories before and after the pulse load are remarkably similar.

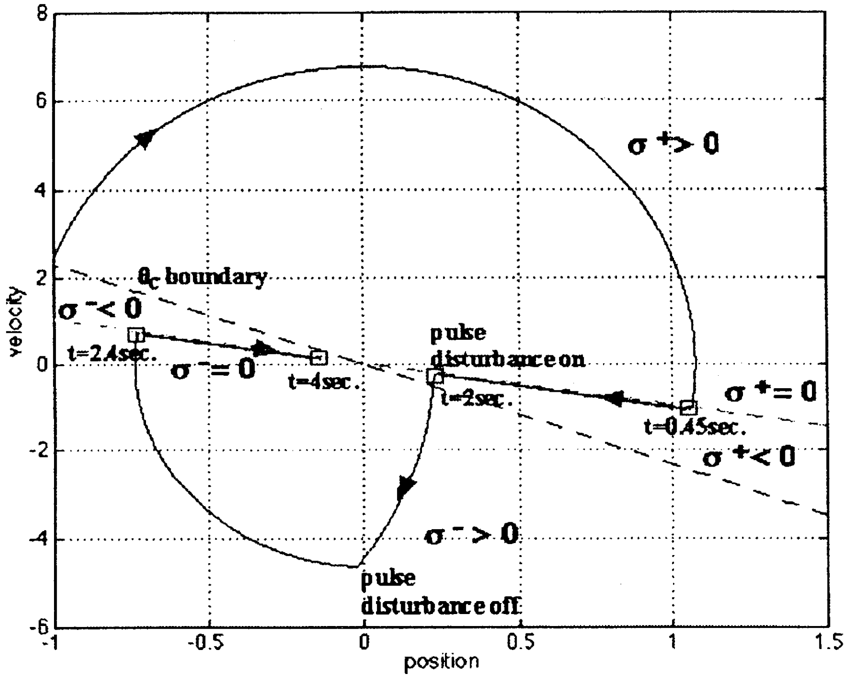

Fig. 3. Polar coordinate based sliding mode phase trajectory (Case 1).

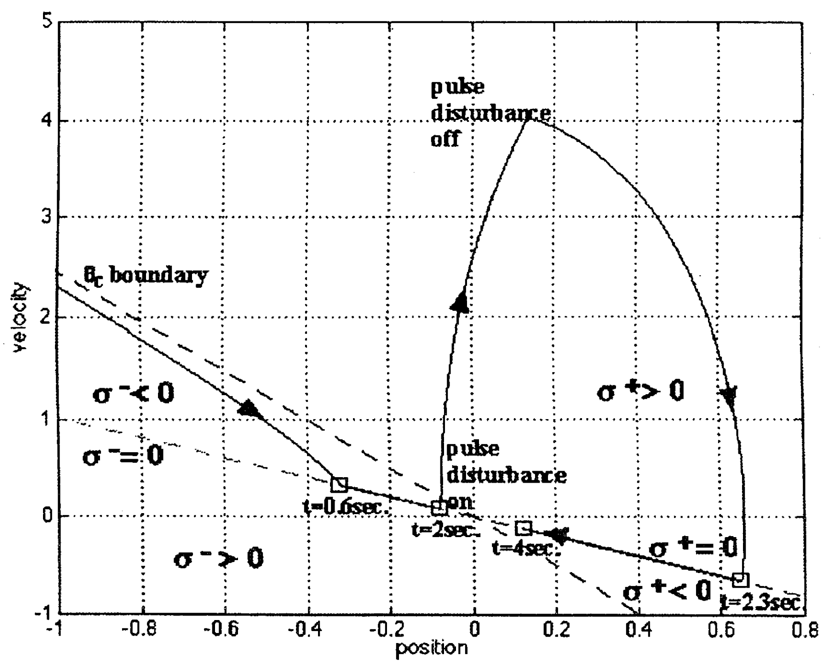

Fig. 4. Polar coordinate based sliding mode phase trajectory (Case 2).

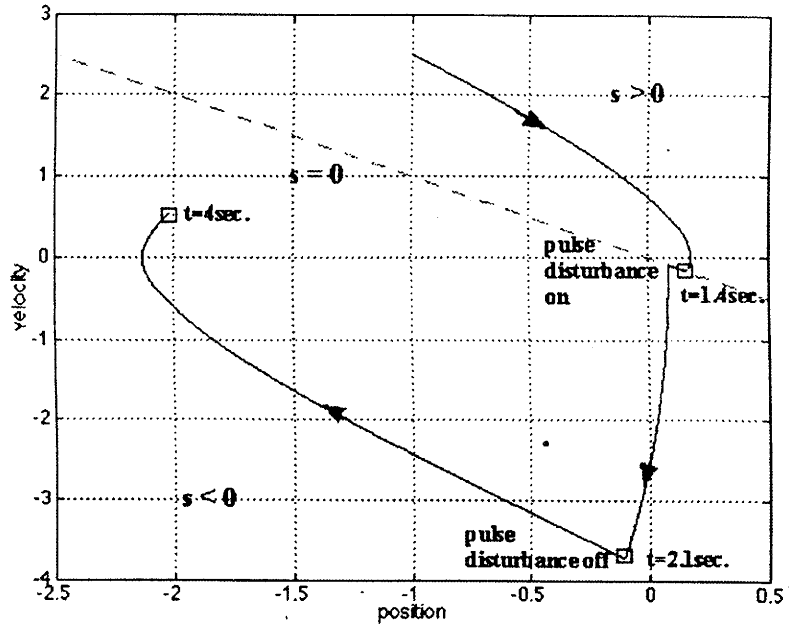

Fig. 5. Classical hyperplane sliding mode phose trajectory (Case 1).

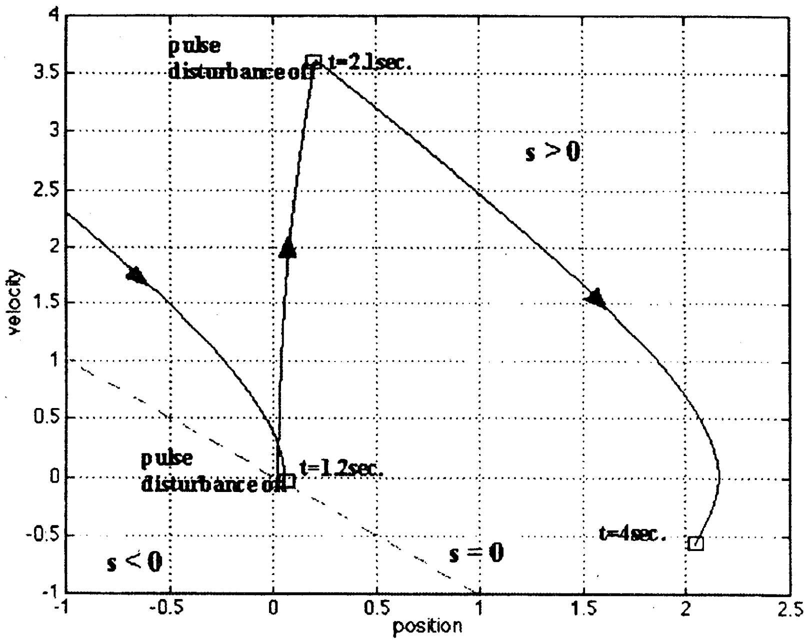

Fig. 6. Classical hyperplane sliding mode phose trajectory (Case 2).

With the additional complexities in the implementation of the polar coordinate based sliding mode control design, the transient performance of the vibratory platform has been shown to be dramatically superior to classical sliding mode control design. Polar coordinate based manifolds offer the advantage of a more flexible adaptation of the manifolds in vibration control problems where different feedback strategies may be required depending on the phase of the oscillation. Furthermore, it allows sliding mode to occur in the preferred quadrants of the phase plane, thus avoiding nonlinear system characteristics due to physical constraints such as hard stops in vibratory platforms.

5. Conclusions

In this paper, we propose a polar coordinate based sliding mode control design approach for solving vibration control problems. This design provides additional flexibility in the design of the sliding mode control law, particularly in the reaching phase. Since different variable structure control laws are devised for different sets of the phase plane, improvements in the overall transient response of the vibration control system over conventional sliding mode controllers with sliding hyperplanes have been shown. While this approach is not easily generalized to other types of linear plants, it does address a wide class of problems related to mechanical systems where the notion of phase has special physical significance.

Acknowledgement

The author would like to acknowledge the discussions with Professor Umit Ozguner of the Ohio State University, Columbus, Ohio, from which the motivations to develop the approach given in this paper were derived.

References

Utkin V.I. (1977): *Variable structure systems with sliding modes.* — IEEE Trans. Automat. Contr., Vol.AC-22, No.2, pp.212–222.

Utkin V.I. (1992): *Sliding Modes in Control Optimization.* — Berlin: Springer-Verlag.

Young K.D. (1993): *Discontinuous control of sliding base isolated structures under earthquakes*, In: Robotics, Mechatronics and Manufacturing Systems, (T. Takamori and K. Tsuchiya, Eds.). — North-Holland: Elsevier Science Publishers B.V., pp.485–490.